RSC Pharmaceutics

ROYAL SOCIETY OF CHEMISTRY

PAPER

View Article Online
View Journal

Cite this: DOI: 10.1039/d4pm00275j

Systematic development and optimization of a microfluidic formulation protocol for liposomal azithromycin

Abdullah A. Masud,[a] Nabilah Ibnat,[a] Areli Medina Hernandez,[a] Kaysi M. Lee,[a] Sophia Li,[a] Ryan Marion,[a] David J. Feola[b] and Vincent J. Venditto *[a]

Delivery of azithromycin *via* liposomal formulation (L-AZM) has been shown to improve the therapeutic index and activity of AZM in a preclinical model of cardiac injury, suggesting strong potential for clinical translation to treat inflammation after a myocardial infarction. However, conventional thin film hydration (TFH) utilized to prepare L-AZM limits its clinical development due to scalability and reproducibility concerns. To overcome these manufacturing challenges, we performed a systematic optimization of the L-AZM formulation utilizing microfluidic nanoprecipitation which has been successfully used for large scale manufacturing of lipid-based therapeutics in a reproducible manner. We adjusted the microfluidic operation parameters and evaluated the resultant liposomes for critical quality attributes (CQAs) of size, polydispersity index (PDI), encapsulation efficiency, and leakage. The optimal flow rate ratio (FRR) and total flow rate (TFR) for the lead formulation was determined to be 4 : 1 and 10 mL min^{-1}, respectively. Utilizing these manufacturing parameters with formulations of different molar ratios resulted in an optimized formulation consisting of DSPC : DSPG : Chol : AZM (1 : 1 : 1 : 0.5) based on the CQAs with decreased size and PDI as compared to TFH. Notably, there is no difference in *in vitro* macrophage polarization activity between the two formulation methods. Collectively, these data guide continued preclinical development as we advance this formulation toward clinical use.

Received 20th September 2024,
Accepted 9th November 2025

DOI: 10.1039/d4pm00275j

rsc.li/RSCPharma

Introduction

Azithromycin (AZM) is a widely used macrolide antibiotic that has also been shown to modulate inflammation in both preclinical[1,2] and clinical settings.[3,4] The benefits of AZM in the context of inflammation are due to the inhibition of inflammatory functions thereby promoting a reparative phenotype in macrophages instead of the classical pro-inflammatory polarization.[2,5–10] However, risk of cardiotoxicity stemming from off-target interactions with ion channels in cardiac muscle cells after systemic administration of AZM poses a serious challenge to its application in managing MI.[1,11] The FDA has also issued a warning for AZM and other macrolides used in patients with inherent cardiac complications due to the risk of arrhythmia and sudden cardiac death.[12] A variety of macrolide formulations have been reported spanning delivery modalities including polymers and liposomes.[13] Notably, incorporation of AZM in a liposomal formulation has been shown to enhance immune cell uptake and mitigate cardiotoxicity in mice after MI, leading to reduced cardiac injury, improved cardiac output, and increased survival.[11] Target oriented delivery of L-AZM also improved the anti-inflammatory efficacy of AZM after an MI by increasing uptake in cells where the drug is known to modulate immune function.[11] Considering the positive outcomes of L-AZM in a murine model of MI, it is critical to develop a scalable and reproducible L-AZM manufacturing protocol for clinical translation.

The emergence of microfluidic formulation technology has caused a paradigm shift in liposome preparation, adding advantageous features in liposome manufacturing, including rapid, automated, and continuous production with reproducible critical quality attributes (CQAs).[14–16] Microfluidic systems utilize fluid dynamic principles for manufacturing liposomes where rapid mixing of an organic solvent with an aqueous solvent in a channel with micron sized dimension causes nanoprecipitation of the lipid components and self-assembly to yield liposomes.[15,17] Thus, continuous flow of the aqueous and organic solvents with lipids and a therapeutic payload enables efficient scalability. Precise control over the flow mixing of the solvents is attainable within the constant geometries of the microfluidic channel, which offers improved repro-

[a]Department of Pharmaceutical Sciences, College of Pharmacy, University of Kentucky, Lexington, KY 40536, USA. E-mail: Vincent.venditto@uky.edu
[b]Department of Pharmacy Practice and Science, College of Pharmacy, University of Kentucky, Lexington, KY 40536, USA

ducibility.[15] Additionally, tuning the flow mixing of the solvents allows improvement in CQAs. For example, decreasing the organic to aqueous solvent ratio leads to smaller liposome size, while flow rate has more dramatic effects on physicochemical properties under high aqueous to organic ratios.[18,19]

Considering the tunability and beneficial features of microfluidics,[15] we systematically optimized a protocol for L-AZM manufacturing by microfluidic preparation. We adjusted the operation parameters (flow rate ratio (FRR) and total flow rate (TFR)) and formulation parameters (lipid composition and AZM concentration) to identify the optimal formulation and manufacturing conditions. Subsequently, we compared the CQAs of the resulting liposomes to find suitable operating conditions ensuring better quality CQAs for L-AZM. Similarly, we investigated the liposome composition by evaluating the liposome's CQAs manufactured using a range of lipid compositions at different molar ratios, along with different AZM concentrations. We then compared our optimized L-AZM formulation prepared by microfluidics with the same formulation prepared by thin film hydration with post-manufacture processing and compared the resulting CQAs. The results from this study move us closer to a scalable and reproducible formulation for clinical translation to treat cardiac inflammation.

Experimental

Reagents

All lipids/phospholipids including 1,2-distearoyl-*sn-glycero*-3-phosphocholine (DSPC), 1,2-distearoyl-*sn-glycero*-3-phospho-1′-*rac*-glycerol, sodium salt (DSPG) and CHEMS (cholesteryl hemisuccinate) were purchased from Avanti Polar Lipids (Alabaster, AL). Cholesterol was re-crystallized in ethanol before being dissolved in ethanol/chloroform for use in formulations. LC-MS grade acetonitrile and methanol were procured from VWR (manufactured by J.T. Baker, Phillipsburg, NJ). Azithromycin dihydrate and monobasic potassium dihydrogen phosphate (KH_2PO_4) were purchased from TCI (Portland, OR) and VWR (manufactured by Amresco LLC., Solon, OH), respectively. Sephadex G-25 (PD-10 column), Snakeskin membrane (MWCO 10 kDa, I.D. 16 mm), ultra-filtration unit (MWCO 30 kDa) were purchased from Cytiva (Marlborough, MA), Thermo Scientific (Waltham, MA), and Pall corporation (Timonium, MD), respectively.

Liposome preparation by microfluidic nanoprecipitation

A commercially available Ignite nano-assembler (Precision NanoSystems Inc., now Cytiva) with NxGen microfluidic technology was employed to prepare liposomal formulations. Liposomes were prepared utilizing published protocols with slight modification.[20] Briefly, the required amount of anionic lipid was first dissolved in 500 μL of an equal mixture (v/v) of DMSO and ethanol at 60 °C in a sonication bath. However, in the case of DSPG, an equimolar amount of HCl to DSPG was added using 2.5 M HCl to enhance the solubility. Subsequently, the required amount of AZM dissolved in 250 μL of DMSO was added to the anionic lipid solution and left to interact at 60 °C for one hour. Then, the required amount of DSPC and cholesterol dissolved in 500 μL of ethanol was added to the anionic lipid and AZM mixture and incubated at 60 °C for 30 min. After the incubation period, liposomes were prepared by mixing the resulting solution with an aqueous solution (HEPES buffer, pH 7.4) using a NxGen microfluidic cassette (Precision NanoSystems, Vancouver, British Columbia). All formulations were prepared at a concentration of 12.8 mM based on combined phospholipid and cholesterol content.

Liposome preparation by thin film hydration

Liposomes were prepared by thin film hydration using an established protocol.[11,21] Briefly, stock solution of lipid and AZM were dissolved in a suitable solvent, whereas DSPC and Cholesterol were dissolved in chloroform, DSPG was dissolved in a mixture of solvents in v/v (chloroform : methanol : DI water = 13 : 6 : 1.6). The lipid mixture was mixed with AZM dissolved in ethanol at various molar ratios described in each figure. A thin film was then prepared by evaporating solvents under reduced pressure using a rotary evaporator. The resulting film was dried overnight under vacuum. Finally, the adequately dried film was re-hydrated with HEPES buffer by sonicating for one hour at 60 °C. Formulations were prepared at a total lipid and cholesterol concentration of 12.8 mM.

Purification of the liposomes to remove unincorporated AZM

Liposomes were purified to remove unencapsulated AZM using three different methods:

(i) *Dialysis* – free AZM and organic solvents were removed by dialyzing liposomes in a chamber prepared from snakeskin membrane (MWCO 10 kDa) against 100 mL HEPES buffer (pH 7.4) with constant stirring at 100 rpm for one hour. Volume of liposome in the dialysis bag was varied between 1.0 mL–3.0 mL based on the increasing mole ratio of total lipid : AZM from 3 : 0.25 to 3 : 2 to avoid oversaturation of AZM and organic solvents in the outside solvent. The volume of the liposome solution collected from the dialysis chamber was used to determine the final concentration of the lipid formulation.

(ii) *Size exclusion column separation* – size exclusion purification of the liposomes was performed according to the published protocol.[21] First, 2.5 mL of the liposome solution was passed through a Sephadex G-25 (PD-10) column (Cytiva, Marlborough, MA) and eluted with 3.5 mL HEPES buffer (pH 7.4). Liposomes eluted starting as the HEPES buffer was added to the column. The complete 3.5 mL volume was collected, and a 1.4-fold dilution factor was used based on manufacturer instructions and confirmed by the final volume of liposomes.

(iii) *Ultrafiltration* – liposomes were purified utilizing a published protocol with slight modification.[22] Briefly, 1 mL of liposome solution was filtered through a commercially available cut-off filter having the MWCO 30 kDa (Pall corporation, Timonium, MD). The liposomes were added to the top chamber of the filter assembly and centrifuged at 810*g* for 25 min to separate free AZM in the bottom chamber from the liposomes retained in the top chamber.

HPLC method for the quantification of liposomal AZM

AZM quantification was performed using a Dionex UPLC Ultimate 3000 (Sunnyvale, CA) equipped with a quaternary pump, autosampler, and a DAD detector. AZM separation was carried out by RP-HPLC using a C18 column (Phenomenex, 100 mm × 4.6 mm, 5 μm, Torrance, CA) with an isocratic mobile phase consisting of 70% acetonitrile and 30% phosphate buffer (pH 7.5). The mobile phase flow rate and detection wavelength were 1 mL min^{-1} and 220 nm, respectively with an injection volume of 20 μL. Under the above-mentioned operating conditions, the AZM peak elution time is ~5 min. To prepare the sample for HPLC analysis, 50 μL of liposomes were dissolved in 950 μL methanol. A standard curve was constructed using AZM solution in methanol with concentrations ranging from 10–400 μg mL^{-1}.

Encapsulation efficiency of AZM in liposomes

The encapsulation efficiency (EE%) of L-AZM was calculated by comparing the total amount of AZM before and after purification. Quantification of AZM was performed by HPLC and pre-and post-purification AZM concentrations were calculated based on a standard curve of AZM. The equation for calculating AZM is:

$$EE\% = \frac{\text{AZM conc. after purification}}{\text{AZM conc. before purification}} \times 100\%$$

Size, polydispersity index, and zeta potential measurement of liposomes

Physical characteristics of the liposomes including size, polydispersity index (PDI), and zeta potential, were measured using either a Zetasizer Pro or Zetasizer Nano ZS (Malvern Panalytical, Westborough, MA). For each formulation, two independent liposome preparations were tested using a 20-fold dilution of liposomes in HEPES buffer (pH 7.4). Size and PDI were determined using ZEN0400 cuvettes with the following settings: four measurements of 15 five second intervals detected at a backscatter angle of 173° at 25 °C. The zeta potential for the liposomes were determined in a DTS1070 folded capillary zeta cell using the following settings: four measurements of at least 50 measurements modelled with the Smoluchowski equation at 25 °C using the automatic settings from the instrument.

Transmission electron microscopy (TEM) of liposomal formulations

Liposomes were characterized by TEM by applying 2 μL of L-AZM formulations to carbon-coated 200 mesh copper grid (Ted Pella, Inc.) and blotted with filter paper. The grid was then stained with phosphotungstic acid, washed with water, dried, and stored in a desiccator until imaging. For imaging, the grid was placed on a single tilt holder and viewed in a Talos F200X Scanning/Transmission Electron Microscope (Thermo Fisher Scientific) using a Field Emission Gun operating at 200 keV. Images were captured digitally using a high speed Ceta Camera and analyzed using Velox Software. Five randomly selected images across the grid were collected and formulations within each image with clearly defined edges were measured.

AZM leakage from liposomes by dialysis

For leakage studies, a portion of purified liposome was added to a dialysis chamber made of snakeskin dialysis membrane (MWCO 10 kDa) and dialyzed against 50 mL HEPES buffer (pH 7.4), maintaining a constant outer temperature of 37 °C and continuous stirring at 60 rpm, based on conditions previously reported for AZM formulations.[23] Volume of liposome in the dialysis bag was varied between 0.25 mL–2.0 mL based on the increasing mole ratio of total lipid : AZM from 3 : 0.25 to 3 : 2 to avoid oversaturation of AZM in the outside solvent. At each sampling point, 1 mL sample was collected from outside the dialysis chamber and replaced with fresh buffer to maintain constant conditions. The collected samples were analyzed for the content of AZM released through the dialysis membrane by HPLC. Sampling was done at 1, 3, 5, 7 and 26 hours of dialysis. Quantification of the AZM content was calculated using a calibration curve constructed within the AZM concentration ranging from 2–70 μg mL^{-1}.

Residual solvent measurement after liposome purification

Gas chromatography with a flame ionization detector (GC-FID) was used to compare the residual ethanol content after purifying L-AZM using three different methods: dialysis, size exclusion column separation, and ultrafiltration. Separation was carried out on an Agilent GC equipped with an Agilent 122-1334 column (30 m × 250 μm × 1.4 μm) in an isothermal process. The sample was held at 60 °C for one minute before the temperature was increased to 110 °C and held for eight minutes. A calibration curve was constructed using ethanol concentrations ranging from 0.6 to 10 μl ml^{-1} in DI water.

The residual DMSO content after L-AZM purification by all three methods was measured using a Dionex HPLC Ultimate 3000 (Sunnyvale, CA) equipped with a quaternary pump, autosampler, and a DAD detector. AZM separation was performed by RP-HPLC using a C4 column (Agilent, 150 mm × 4.6 mm, 5 μm) with an isocratic mobile phase consisting of DI water. The mobile phase flow rate was 0.5 mL min^{-1}, and the detection wavelength was 254 nm, with an injection volume of 20 μL. A calibration curve was constructed using DMSO concentrations ranging from 1.0 to 200 nL mL^{-1} in DI water.

In vitro activity and cell viability

J774A.1 murine macrophages (ATCC) were cultured to confluency in DMEM with 10% FBS and 1% penicillin/streptomycin at 37 °C in 5% CO_2. Once confluent, the cells were scraped, counted, and plated at a density of 2.5×10^4 cells per 100 μL of media in 96-well plates. The plated cells were treated with interferon (IFN)-γ (final concentration 100 ng mL^{-1}). Selected wells were treated with F-AZM, empty liposomes, or L-AZM prepared by microfluidics or thin film hydration (AZM concentration 0–135 μM). Cells were incubated overnight at 37 °C in 5% CO_2 before stimulation with lipopolysaccharide (LPS) and

incubated for 24 h. The cells were then centrifuged at 1200*g* for 5 min. Half of the media supernatant was collected for cytokine analyses, while the cells and remaining media was analyzed for cell viability. IL-12 concentrations were measured using 10 μL media from each well and quantified by sandwich ELISA according to manufacturer's instructions (BioLegend). Cell viability assessed by MTS assay (Promega) by adding 20 μL MTS reagent to each well. The assay plate was incubated for 4 h at 37 °C and absorbance measured at 490 nm (BioTek Synergy H1).

Statistical analysis

GraphPad Prism (GraphPad Software, La Jolla, CA) was utilized for plotting the figures and performing statistical analyses. To compare liposome sizes and EE% of the L-AZM formulations, one-way ANOVA with Tukey's test for multiple comparisons were used. Statistical analysis for leakage was performed by one-way ANOVA compared to F-AZM with Dunnett's multiple comparisons test. For comparing, liposome sizes and EE% of the optimized L-AZM formulation manufactured by microfluidics and thin film hydration with purification by dialysis, column separation and ultrafiltration, two-way ANOVA with Šídák's multiple comparisons was used. Statistical comparisons over time for stability studies used two-way ANOVA with Geisser–Greenhouse multiple comparisons. The *p*-value cut-offs for statistical significance are $*p < 0.05$, $**p < 0.01$, $***p < 0.001$ and $****p < 0.0001$. All average values are presented as mean ± standard deviation (SD). In addition, AZM leakage rates of different L-AZM formulations were also compared by calculating similarity factors ($f2$) and difference factors ($f1$) using industry guidance from the FDA.[24] Leakage rates were considered similar when $50 \leq f2 \leq 100$ or $0 \leq f1 \leq 15$.

Results

Microfluidic optimization of manufacturing parameters for L-AZM

The microfluidic operation parameters total flow rate (TFR) and flow rate ratio (FRR) dictate the physicochemical properties of liposomes;[16,25,26] therefore, we first opted to optimize these two parameters. To do so, we used our parent formulation composed of an equal molar mixture of DSPC, DSPG, and cholesterol (1 : 1 : 1) based on evidence of immunomodulation using *in vivo*[11] and *in vitro* models.[21] To examine the effect of TFR, L-AZM formulations were prepared using different TFR between 5–20 mL min^{-1} while maintaining a constant FRR at 4 : 1 (aqueous to organic). The sizes of the resultant liposomes exhibited minimal variation of 160–180 nm, with all PDI values <0.1 (Fig. 1A). Although there were no significant differences observed between size and PDI when using different TFRs, encapsulation efficiency (EE%) decreased from 81 ± 5% at 5 mL min^{-1} and 76 ± 0.2% at 10 mL min^{-1} to 62 ± 2% for 20 mL min^{-1} (Fig. 1B).

The effect of FRR was also assessed using aqueous : organic ratios of 2 : 1, 3 : 1, 4 : 1, and 5 : 1 while keeping the TFR constant at 10 mL min^{-1}. Under these conditions, increasing FRR resulted in decreasing liposome diameters from 240 nm to 150 nm, with a consistent PDI range (<0.2) across all FRR (Fig. 1C). EE% was found to be within a close range of 69–76% without any significant difference among the FRRs used (Fig. 1D). Therefore, the optimal conditions used for further experiments are a TFR of 10 mL min^{-1} and FRR of 4 : 1, based on the optimal rate at which formulations could be reproducibly manufactured at ideal size, PDI, and encapsulation efficiency.

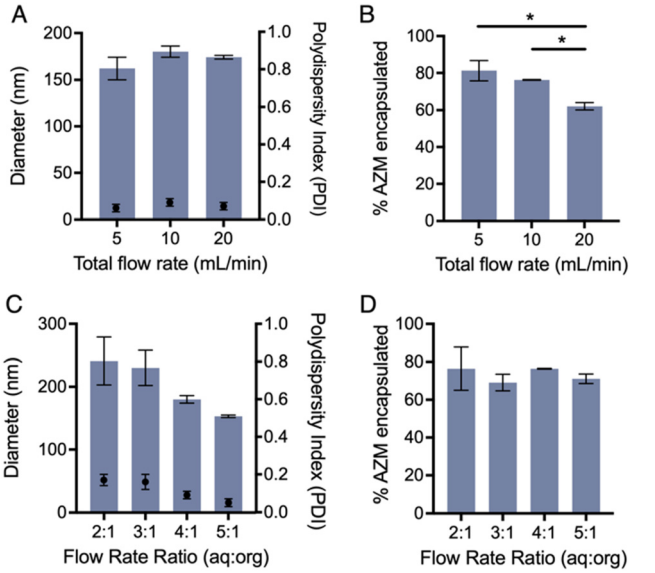

Fig. 1 Effect of the microfluidic total flow rate (TFR) and flow rate ratio on the physicochemical properties of L-AZM. (A and B) Liposomes were prepared using (A and B) variable TFR while flow rate ratio (FRR) was constant at 4 : 1 (aqueous : organic), or (C and D) variable FRR while total flow rate (TFR) was constant at 10 mL min^{-1}. Lipid composition was DSPC : DSPG : Chol : AZM (1 : 1 : 1 : 0.5) at 12.8 mM with HEPES buffer (pH 7.4) used as the aqueous phase. The resulting liposomes were purified *via* dialysis against HEPES buffer pH 7.4. (A and C) Size and PDI, and (B and D) encapsulation efficiencies of the resulting formulations are shown. Experiments were performed in triplicate on two different days for a total of six replicates. Results are presented as mean ± SD. Statistical analysis for encapsulation efficiencies performed by one-way ANOVA with Tukey's multiple comparisons. Significant differences are expressed as $*p < 0.05$.

Optimization of lipid composition for L-AZM

Using the optimized TFR and FRR, we further extended the optimization process for lipid composition, another critical parameter that controls the physicochemical properties of the liposome. As mentioned, we initially used our parent formulation composed of DSPC : DSPG : Chol : AZM (1 : 1 : 1 : 0.5) for the microfluidic optimization. DSPG is an anionic lipid with a negatively charged phosphate group, potentially ion pairing with the bi-cationic AZM,[27] while DSPC and cholesterol (Chol) are helper lipids that facilitate the stability of liposomes.[28] In an attempt to further simplify the formulation, we investigated the utility of cholesteryl hemisuccinate as a replacement for

both DSPG and Chol by including an anionic derivative of cholesterol. Cholesteryl hemisuccinate (CHEMS) is a widely used anionic lipid capable of increasing bilayer fluidity similar to cholesterol.[22] In exploring the superior lipid composition for L-AZM, five different formulations were prepared using DSPG and CHEMS alone or in combinations (MF1–MF5) (Fig. 2A). Initial content of AZM (2.1 mM) and total lipid (12.8 mM) are identical for all five formulations. AZM is bi-cationic (charge, +2), and both DSPG and CHEMS have a single anionic group (charge, −1); thus, based on the molar ratio, the negative to positive charge ratio is 1 : 1 for MF1, MF2, and MF3. In contrast, the charge ratio is 2 : 1 for MF4 and 0 : 1 for control (MF5). All formulations were prepared using the optimized microfluidic operation parameters, TFR 10 mL min^{-1} and FRR 4 : 1.

The size and PDI of the resulting liposomes are displayed in Fig. 2B. Liposomes containing anionic lipids (MF1, MF2, MF3, MF4) are larger in size than the control, MF5, having no anionic lipids. While the size of MF5 is the lowest, 96 ± 4 nm, the largest size of 380 ± 19 nm was observed for MF4, which contained the highest amount of anionic lipid among all five formulations. The remaining three formulations (MF1, MF2, MF3), exhibit liposome diameters within a close range of 180–230 nm. Notably, formulations containing DSPG and CHEMS together exhibit the highest PDI (MF2, 0.5; MF4, 0.6). The total Chol content of MF2 is 17 mol% compared to the other formulations containing 33 mol% Chol or CHEMS, potentially leading to the increased PDI, however similar results are observed with MF4 suggesting an inherent issue with ion pairing using CHEMS. Formulations containing only DSPG (MF1) or CHEMS (MF3) result in PDI ≤ 0.2. HPLC quantification of AZM before and after dialysis reveals no significant difference in EE% for each formulation. The EE% of MF1 (76 ± 0.2%), MF2 (74 ± 0.6%), MF4 (82 ± 1%) are only slightly elevated above the neutral formulation MF5 (67 ± 4%) and the CHEMS-only formulation, MF3 (67 ± 11%) (Fig. 2C).

In addition to size, PDI, and EE%, we studied the AZM release profile of all five liposomes over 24 h using dialysis. Multi-time point quantification of AZM leakage from the dialysis chamber generated the drug release profile shown in Fig. 2D. Despite almost similar EE%, MF3, which contains only CHEMS as the anionic lipid component exhibited release rates similar to free AZM or control non-anionic liposomes (MF5). The other three formulations which contain DSPG as a portion of their makeup (MF1, MF2, and MF4), showed relatively slower release. To further compare leakage rates of each formulation we calculated the difference factor ($f1$) and similarity factors ($f2$) for each formulation. The similarity and difference factors are the FDA recommended statistical models to estimate similarity in tablet dissolution rates[24] and have also been adapted for liposomal formulations.[29] Given the parallel values obtained for $f1$ and $f2$ for each comparison, only $f2$ values are shown (Fig. 2E). An $f2$ value between 50–100 signifies similarity in drug release rates.[30] In alignment with the one-way ANOVA analysis of leakage rates, the control formulation lacking anionic lipid (MF5) is similar to both the CHEMS containing formulation (MF3: $f2$ = 55) and free AZM (F-AZM: $f2$ = 50) (Fig. 2E). Formulations MF1, MF2, and MF4 are all significantly different from free AZM based on ANOVA and $f2$ analysis indicates MF1 and MF2 are similar in leakage ($f2$ = 75). However, the high PDI values of MF2 and MF4 preclude further development of these formulations and positions MF1 as a lead candidate for further investigation.

A

	Formulation component (*charge*)					Charge Ratio (-/+)
	DSPC (0)	DSPG (-1)	CHOL (0)	CHEMS (-1)	AZM (+2)	
MF1	1	1	1	-	0.5	1:1
MF2	2	0.5	-	0.5	0.5	1:1
MF3	2	-	-	1	0.5	1:1
MF4	1	1	-	1	0.5	2:1
MF5	2	-	1	-	0.5	0:1

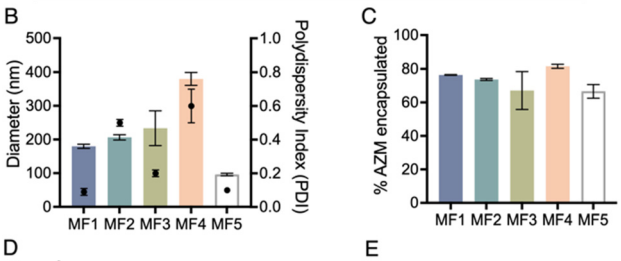

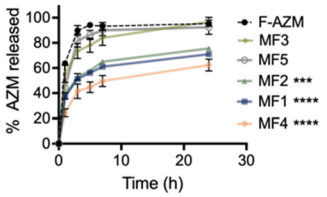

E

	F-AZM	MF1	MF2	MF3	MF4
MF1	24				
MF2	26	75			
MF3	47	32	35		
MF4	18	48	44	24	
MF5	50	30	32	55	22

Fig. 2 Optimization of the lipid composition for L-AZM. (A) Five L-AZM formulations (MF1–MF5) were designed with varying molar ratios of anionic lipids (DSPG and CHEMS) and helper lipids (DSPC and Chol). Formulations were prepared using the optimized microfluidic operation parameters (TFR: 10 mL min^{-1}; FRR: 4 : 1) in HEPES buffer (pH 7.4) as aqueous phase. The resulting formulations were purified *via* dialysis against HEPES buffer pH 7.4. (B) Size and PDI; (C) encapsulation efficiencies; (D) drug leakage profiles; and (E) calculated similarity factors ($f2$) shown with values greater than 50 shaded to indicate similarity in release rates of the resulting liposomes. Experiments were performed in triplicate on two different days for a total of six replicates. Results are shown as mean ± SD. Statistical analysis for encapsulation efficiencies performed by one-way ANOVA with Tukey's multiple comparisons test. Statistical analysis for leakage performed by one-way ANOVA compared to F-AZM with Dunnett's multiple comparisons test. Significant differences are expressed as ***p < 0.001 and ****p < 0.0001.

Optimizing azithromycin concentration in L-AZM

After optimizing for lipid composition with constant drug loading, the AZM content was then optimized by adjusting AZM concentration relative to constant lipid composition (Fig. 3). Five formulations were prepared using increasing concentrations of AZM within the optimized formulation DSPC : DSPG : Chol (1 : 1 : 1) (Fig. 3A). This lipid composition matches our parent formulation (PF),[11,21] which we previously used for *in vivo* and *in vitro* studies, they are denoted as PF1–PF5. The mole ratio of DSPG : AZM varied from 1 : 0.25 to 1 : 2.0 corresponding to AZM concentrations of 1.07–8.5 mM.

A

	Formulation component (*charge*)				Charge Ratio (-/+)
	DSPC (0)	DSPG (-1)	CHOL (0)	AZM (+2)	
PF1	1	1	1	0.25	1:0.5
PF2	1	1	1	0.50	1:1.0
PF3	1	1	1	0.75	1:1.5
PF4	1	1	1	1.00	1:2.0
PF5	1	1	1	2.00	1:4.0

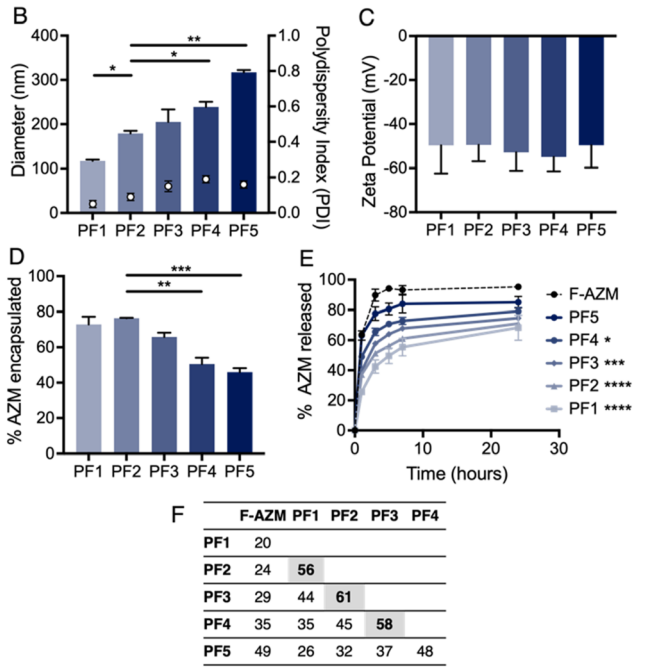

F

	F-AZM	PF1	PF2	PF3	PF4
PF1	20				
PF2	24	**56**			
PF3	29	44	**61**		
PF4	35	35	45	**58**	
PF5	49	26	32	37	48

Fig. 3 Optimization of AZM concentration in L-AZM. (A) Five L-AZM formulations (PF1–PF5) were designed with varying molar ratios of AZM relative to anionic lipid. Formulations were prepared using the optimized microfluidic operation parameters (TFR: 10 mL min^{-1}; FRR: 4 : 1) in HEPES buffer (pH 7.4) as aqueous phase. The resulting formulations were purified *via* dialysis against HEPES buffer pH 7.4. (B) Size and PDI; (C) zeta potential; (D) encapsulation efficiencies; (E) drug leakage profiles; and (F) calculated similarity factors (*f*2) shown with values greater than 50 shaded to indicate similarity in release rates of the resulting liposomes. Experiments were performed in triplicate on two different days for a total of six replicates. Results are shown as mean ± SD. Statistical analysis for sizes and encapsulation efficiencies performed by one-way ANOVA with Tukey's multiple comparisons test. Statistical analysis for leakage performed by one-way ANOVA compared to F-AZM with Dunnett's multiple comparisons test. Significant differences are expressed as *$p < 0.05$, **$p < 0.01$, ***$p < 0.001$, ****$p < 0.0001$.

All liposomes were prepared using optimized microfluidic operation parameters and evaluated for their physicochemical characteristics.

The size and PDI of the liposomes follow an increasing trend with the increased mole ratio of AZM (Fig. 3B). PF1 exhibits the lowest mole ratio of DSPG : AZM (1 : 0.25) and forms the smallest liposomes (117 ± 3 nm), and liposomes steadily increased to nearly three times larger with the highest concentration of AZM (PF5, 317 ± 5 nm). Although PDI follows an increasing trend with additional AZM in liposomes, PDI did not surpass 0.2 for any formulation. In addition to size and PDI, the surface charge of each formulation indicated minimal variation between formulation with no clear trend in surface charge observed (zeta potential: −50 to −55 mV; Fig. 3C). Counter to trends observed with size and PDI, EE% of the liposomes generally exhibit a decreasing trend with the increased mole ratio of AZM (Fig. 3D). The exception to this trend is that PF1 and PF2 have charge ratios of 1 : 0.5 and 1 : 1, respectively and exhibit similar EE% of 73 ± 4% and 76 ± 0.2, respectively. From the optimal formulations (PF1 and PF2) EE% decreases to 66 ± 2% (PF3), 51 ± 4% (PF4) and 46 ± 2% (PF5) as AZM content increases.

Leakage studies also demonstrate that AZM is released at a faster rate with increasing concentration in the formulation (Fig. 3E). The release rate of the formulations followed an increasing trend from PF1 to PF5, although the release rates of formulations with the lowest concentrations of AZM (PF1, PF2) are similar. While PF1 exhibits only 29 ± 2% AZM release in the first hour, 66 ± 3% is released from PF5 within the same time frame. Nearly all AZM is released from PF5 within 3 hours with a release profile statistically faster than all other formulations. Similarity factor (*f*2) calculations (Fig. 3F) also reflect differences observed by one-way ANOVA in which increasing concentration of AZM reduced the significant differences when compared to free AZM. Given the stepwise nature of AZM concentration and corresponding leakage rate for each formulation, PF1 is similar to PF2 (*f*2 = 56), PF2 is similar to PF3 (*f*2 = 61), and PF3 is similar to PF4 (*f*2 = 58). Additionally, free AZM is least similar to PF1 (*f*2 = 20) and PF2 (*f*2 = 24) corresponding with the lowest AZM leakage (Fig. 3F).

Comparison of liposomes prepared by microfluidics and thin film hydration

Finally, liposomes prepared by microfluidics and conventional thin film hydration methods were compared. In doing so, liposomes made using the optimized formulation (PF2) employing the above-mentioned methods were compared based on physicochemical properties. To undergo a robust comparison, we performed post-manufacturing processing of the liposomes to remove unincorporated AZM using three different methods: dialysis, size exclusion column separation, and ultrafiltration. Notably, regardless of post-purification processing technique utilized, L-AZM prepared by microfluidics exhibited improved size and PDI relative to those made by thin film hydration (Fig. 4A). The diameter of the microfluidic based L-AZM is ~160 nm for all three post-manufacturing methods compared to 220–290 nm for liposomes prepared by thin film hydration. Similarly, PDI was consistently 0.1 for microfluidic preparations and increased to 0.2–0.4 for all thin film hydration preparations. The combination of thin film hydration followed by dialysis yielded the largest liposomes (289 nm) and the highest PDI (0.4). On the other hand, EE% of L-AZM prepared by microfluidics and thin film hydration are comparable irrespective of the post-manufacturing methods utilized (Fig. 4B). However, differences in EE% were observed depending on the method utilized to purify them with dialysis and ultrafiltration resulting in similar EE% of 81–85%, which dropped to 67% for size exclusion column separation.

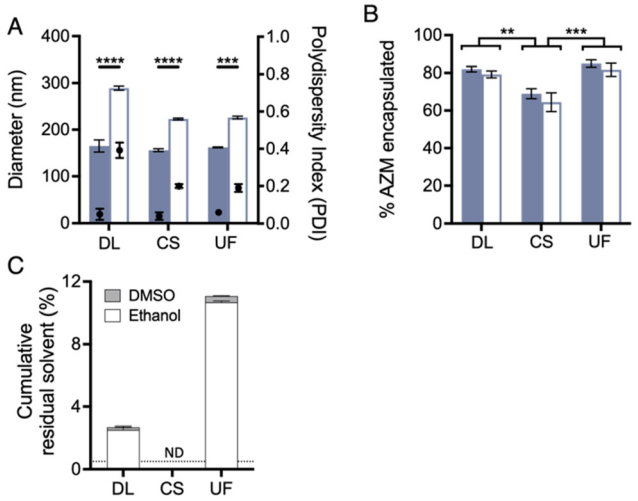

Fig. 4 Comparison of microfluidic and thin film hydration with post manufacture processing. Liposomes were prepared by microfluidics or thin film hydration using the optimized composition (DSPC : DSPG : Chol : AZM = 1 : 1 : 1 : 0.5). Formulations prepared by microfluidics use the optimized microfluidic operation parameters (TFR: 10 mL min^{-1}; FRR: 4 : 1) in HEPES buffer (pH 7.4) as aqueous phase. The resulting formulations were processed *via* three different methods (dialysis (DL), column separation (CS), and ultrafiltration (UF)) and characterized for their (A) size and PDI; and (B) encapsulation efficiencies. Microfluidics are represented in solid blue bars and thin film hydration represented in white bars with blue border. (C) Residual solvent was analyzed by gas chromatography and HPLC to quantify ethanol and DMSO, respectively. Dashed line represents the maximal allowable concentration limit (0.5%). ND = not detected. Experiments were performed in triplicate on two different days for a total of four to six replicates. Results are shown as mean ± SD. Statistical analysis for liposome sizes and encapsulation efficiencies performed by two-way ANOVA with Šídák's multiple comparisons. Significant differences are expressed as $^{**}p < 0.01$, $^{***}p < 0.001$, $^{****}p < 0.0001$.

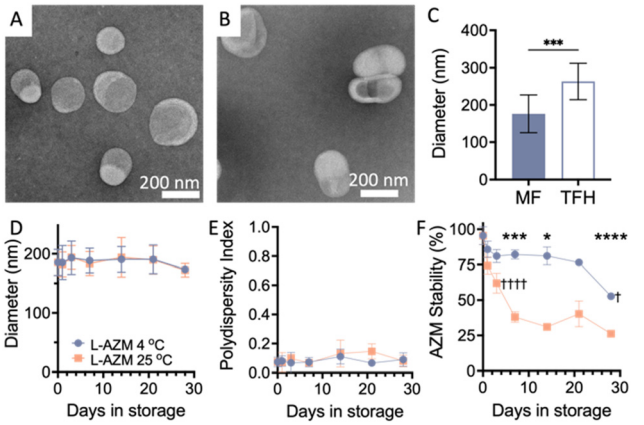

Fig. 5 Transmission electron microscopy and storage stability of L-AZM formulations. Liposomes were prepared by microfluidics or thin film hydration using the optimized composition (DSPC : DSPG : Chol : AZM = 1 : 1 : 1 : 0.5), microfluidic parameters (TFR: 10 mL min^{-1}; FRR: 4 : 1) in HEPES buffer (pH 7.4) as aqueous phase and processed *via* dialysis. (A) Representative TEM image of formulations prepared by microfluidics; (B) representative TEM image of formulations prepared by thin film hydration; (C) quantification of formulations prepared by both methods. Microfluidic formulations were then analyzed over time when stored at 4 °C and 25 °C with (D) size, (E) PDI, and (F) AZM stability shown. Results shown as mean ± SD, number of independent batches (n = 3). Statistical analysis for liposome sizes and encapsulation efficiencies in (C) performed by t-test. Statistical analysis in (F) performed by two-way ANOVA with Geisser–Greenhouse correction and Tukey's multiple comparisons for time-based effects within groups, and Sidak's multiple comparisons for group differences. Significant differences are expressed as $^{*}p < 0.05$, $^{***}p < 0.001$, $^{****}p < 0.0001$ for intergroup comparisons, while $^{\dagger}p < 0.05$, and $^{\dagger\dagger\dagger}p < 0.001$ are used for intragroup comparisons relative to time 0.

Given our use of organic solvents and the necessity to reduce their concentration when used in biological systems, we compared the efficiency of three purification methods in removing ethanol and DMSO after microfluidic preparation. The FDA maximum allowed residual solvent level is 0.5% (5000 ppm). Therefore, we employed GC-FID and HPLC to measure the residual ethanol and DMSO, respectively, after L-AZM purification. Although the theoretical initial residual solvent content is approximately 20% (8% DMSO and 12% ethanol), we found that the size exclusion method was most effective in removing these solvents. The size exclusion PD-10 column removed the residual solvents to undetectable levels, whereas the ultrafiltration method retained about 11%, and dialysis retained 2.7% organic solvent concentrations (Fig. 4C).

Assessment of liposomal formulations by transmission electron microscopy

The optimized formulations were then prepared by thin film hydration and microfluidics and visualized by transmission electron microscopy (TEM) (Fig. 5). Liposomes were best visualized using phosphotungstic acid as a negative stain. Using TEM, liposomes prepared by microfluidics have average diameter of 176 ± 51 nm, while liposomes prepared by thin film hydration have a size of 263 ± 49 nm. These data are in alignment with the data generated in solution phase by dynamic light scattering (Fig. 4A).

Assessment of liposome stability over time

Microfluidic formulations were then analyzed over time for size PDI and drug stability when stored at 4 °C and 25 °C for 28 days (Fig. 5D–F). While there are no changes in size or PDI when formulations are stored at either temperature, AZM stability decreases as determined by HPLC. In this case, free drug is not removed from formulations and the observed decrease in AZM is likely due to degradation.[31] When stored at 4 °C, there is a statistically significant decrease to 52 ± 1% AZM content at 28 days as compared to 62 ± 7% decrease in just 3 days when stored at 25 °C. Notably, there is a non-significant decrease in AZM content when stored at 4 °C from 86 ± 6% at 1 day to 77 ± 2% at day 21. A statistical difference between storage conditions is first observed at 7 days of storage when formulations stored at 4 °C exhibit 82 ± 5% as compared to 38 ± 4% when stored at 25 °C. These data suggest that while the formulations remain stable, the loss of AZM is likely due to degradation as described in the literature,[31] and

in alignment with the FDA-approved prescribing information for clinical AZM preparations.[32]

In vitro assessment of L-AZM formulations

The optimization approach for L-AZM is driven by the potential for clinical use. We have previously demonstrated the ability of L-AZM to modulate immune responses after a myocardial infarction in mice through cardiac and systemic reduction in pro-inflammatory markers, reduced cardiac fibrosis and improved survival.[11] L-AZM achieves its immunomodulatory effect through inhibition of NFκB signaling.[8] Therefore, we quantified cell viability and pro-inflammatory IL-12 production in J774A.1 murine macrophages treated with F-AZM, empty liposomes, and L-AZM prepared by thin film hydration and microfluidics. F-AZM exhibits reduced cell viability at concentrations greater than 40 μM, while L-AZM prepared by either thin film hydration or microfluidics exhibits reduced cell viability at AZM concentrations greater than 90 μM (Fig. 6A). Notably, F-AZM exhibits 9.1 ± 5.9% cell viability at 90 μM as compared to 80.5 ± 10.4% for MF (p = <0.0001), 82.2 ± 3.6% for TF (p = <0.0001), and 85.8 ± 1.3% for empty liposomes (p = <0.0001). Importantly, there is no observable toxicity with empty liposomes at all concentrations tested.

The efficacy of each formulation to reduce IL-12 production relative to control LPS stimulated J774A.1 murine macrophages was then assessed. LPS stimulated J774A.1 macrophages produce 2.2 ± 0.1 ng mL^{-1} IL-12 in the media, which is fractionally increased with empty liposomes (Fig. 6B). Comparison of IL-12 reduction at the highest non-cytotoxic AZM concentration results in 55.9 ± 6.8% reduction for F-AZM at (40 μM AZM), 99.2 ± 4.6% reduction for MF (90 μM AZM), and 95.8 ± 8.9% reduction for TF (90 μM AZM). Notably, there is no significant difference between MF and TF prepared L-AZM formulations. These data indicate a significant reduction in cytotoxicity and improved *in vitro* efficacy when incorporated in a liposomal bilayer.

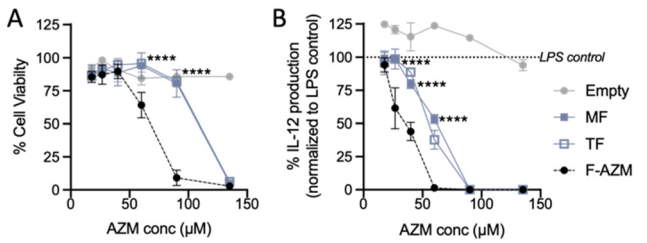

Fig. 6 *In vitro* assessment of azithromycin in murine macrophages. Optimized formulations were used to treat pro-inflammatory J774A.1 murine macrophages as compared to F-AZM and empty liposomes and normalized to untreated pro-inflammatory control cells receiving only IFN-γ and LPS (denoted by dashed line). (A) Cell viability as determined by MTS assay at increasing concentrations of AZM. (B) Relative IL-12 concentration in media. Results shown as mean ± SD, number of independent batches (n = 3). Statistical analysis performed by two-way ANOVA with Geisser–Greenhouse correction and Sidak's multiple comparisons for group differences. Significant differences are expressed as ****p < 0.0001 to indicate concentration dependent comparisons between MF and F-AZM.

Discussion

Microfluidic preparation of L-AZM provides a route to clinical utility by improving scalable and reproducible manufacturing. Through optimization of the microfluidic parameters (FRR = 4 : 1; TFR = 10 mL min^{-1}) using a charge-paired formulation between AZM and DSPG results in a formulation containing DSPC : DSPG : Chol : AZM (1 : 1 : 1 : 0.5) with optimal CQAs including liposome diameter <200 nm and PDI <0.2. The formulations also exhibit stability over time, but AZM degradation limits shelf-life, which is also observed with clinical preparations of AZM.[31,32] The optimized protocol described here supports continued preclinical development with the goal of clinical translation.

Stable liposomal formulations are dependent on many factors including lipid composition, manufacturing protocols, and drug properties. L-AZM has been reported before for its anti-microbial activity based on a thin film hydration manufacturing protocol,[22,23,33–38] which is not ideal for large-scale manufacturing due to significant labor and reproducibility challenges.[15] Nevertheless, we previously employed a thin film hydration strategy to investigate the immunomodulatory activity of L-AZM in the context of myocardial infarction.[11] Generating L-AZM by microfluidics builds upon prior data with thin film hydration as well as evidence of optimal microfluidic parameters for other active ingredients. In general, changes in TFR have minimal effect on the particle size and PDI,[14,19,26] while changes in FRR lead to more dramatic effects on physicochemical parameters.[16,19,25] Notably, in our system FRR and TFR demonstrate modest effects on the lead candidate formulation with a trend toward smaller size with increasing FRR. More importantly, a low FRR results in increased variability between preparations suggesting that a higher ratio (4 : 1 or 5 : 1) is ideal for L-AZM. When considering TFR, size and PDI of the formulations are similar, but EE% of L-AZM is reduced significantly when using the highest TFR (20 mL min^{-1}). Although microfluidic parameters are not universally applicable, our optimized parameters (TFR: 10 mL min^{-1}; FRR: 4 : 1) are similar to optimized parameters for other liposomal formulations.[39]

AZM incorporation in the liposomes is also reliant on the physicochemical characteristics of the components including the partition coefficient (log P) of the drug, the lipid charge, and membrane fluidity.[28] Thus, optimizing phospholipid ratio is vital to ensure suitable CQAs of the liposomal formulations. Lipophilic molecules having a high partition coefficient (log P > 5.0) are stably incorporated in the bilayer while highly hydrophilic molecules (log P < 1.7) incorporate stably in the aqueous core.[40] AZM possesses a midrange log P of 2.7 causing it to partition between bilayer and the aqueous phases making it a challenging molecule to encapsulate. Because of this, small changes in lipid content led to significant variability in the release profile. Therefore, by utilizing electrostatic ion pairing between anionic lipids and AZM provides an effective strategy to enhance the formulation stability of L-AZM.[22,27] Our current studies demonstrate that incorporation of anionic lipids

(DSPG, CHEMS) in the formulation have little effect on encapsulation efficiency, but enhance the retention of AZM in the formulation. Notably, DSPG appears to be a more efficient ion pair with AZM as compared to CHEMS as evidenced by superior CQAs of L-AZM formulations containing DSPG.

An overall assessment of the CQAs indicates that DSPC : DSPG : Chol (1 : 1 : 1) is the best composition for L-AZM. This formulation is based in-part on prior evidence of this formulation for use as an antimicrobial agent, and for immune modulation based on a library of formulations.[21,33] In contrast to our microfluidics results that demonstrate CHEMS to be less efficient at ion pairing with AZM, previous work by Ren *et al.* and Geng *et al*. indicate more stable ion pairing of CHEMS with macrolides.[22,41] However, they used a multistep process to make the liposomes in which AZM and CHEMS are first incubated at freezing temperature overnight, followed by solvent evaporation resulting in a CHEMS–AZM powder which is then mixed with other lipids in an organic solvent to generate a thin film for rehydration.[22,41] The incubation of AZM with CHEMS at low temperatures might be the key driving force for their successful ion pairing. Therefore, the relatively short incubation between CHEMS and AZM described in this study might not be sufficient for optimized ion pairing. However, including such a step in the manufacturing process further complicates the scalability of the formulation and was not investigated further.

Maximizing the EE% of nanoparticles is beneficial for many reasons including overall dose and minimization of drug waste which can ultimately reduce manufacturing costs.[42] The lead L-AZM candidate exhibits 76% drug loading efficiency, while producing relatively slower drug release over a period of 24 hours as compared to other L-AZM formulations studied here. Although a pharmacokinetic study of L-AZM has not been completed, it is known that circulation half-life in naïve, wild-type mice using non-PEGylated liposomes is ~4 h, as compared to ~11 h for PEGylated formulations.[43] Importantly, L-AZM is designed as a non-PEGylated formulation to promote uptake by immune cells trafficking to sites of inflammation.[11] Therefore, we hypothesize that a circulation half-life of ~1–2 hours in mice suffering a cardiac injury should provide a pharmacokinetic profile that minimizes off-target cell uptake in cardiomyocytes. Our studies that demonstrate cardioprotection in mice suffering from myocardial infarction supports this.[11] With an optimized formulation and manufacturing protocol, complete pharmacokinetic and biodistribution studies will be conducted in both murine and large animal models.

Finally, comparing the microfluidic formulation with thin film hydration methods along with post-manufacture processing provides a clear indication of the ideal manufacturing approach for clinical translation. Liposome purification is also an important step of the manufacturing process and established methods are known to alter the liposome properties.[22,37] Thus, a robust evaluation is required using a multi-method comparison. Notably, an overall improvement in the size and PDI of L-AZM is observed when microfluidic preparation is used as compared to thin film hydration, regardless of the purification method employed, which is indicative of the superiority of the microfluidic system over conventional liposome preparation methods. While a comparable EE% is observed between formulation techniques, size exclusion column purification results in a significant decrease in EE% as compared to dialysis and ultracentrifugation, which is consistent with previous reports.[22,37] These data correspond with removal of residual solvents below the permissible daily exposure (PDE) level in formulations. According to the International Conference on Harmonization (ICH Q3C-R9: Impurities: Guideline for Residual Solvents), both ethanol and DMSO are class 3 solvents, which have low toxic potential with a maximum allowable concentration limit of 0.5% (5000 ppm), which is efficiently achieved with size exclusion column separation, but not with ultrafiltration or dialysis. Nonetheless, there are no differences when comparing the *in vitro* macrophage polarization activity or the reduced cytotoxicity between microfluidic and thin film hydration preparations, which are both significant improvements over F-AZM, and supports continued preclinical development of L-AZM to treat acute inflammatory conditions.

Conclusions

Liposomes are an ideal strategy to improve the therapeutic index of AZM for use as an immunomodulatory agent in the context of cardiac inflammation given the risk of cardiac toxicity in subjects experiencing a heart attack. Herein, we describe the systematic optimization of L-AZM manufacturing using microfluidic nanoprecipitation to identify the optimal TFR and FRR of the microfluidic system as well as the optimal lipid components and AZM concentration in the formulation. By optimizing the microfluidic operation parameters and liposomal composition, an optimized L-AZM formulation is achieved with optimal CQAs for clinical translation. Continued efforts focused on sterile manufacturing, long-term stability, and *in vivo* studies focused on pharmacokinetic profiles and efficacy in a large animal model will position L-AZM for clinical translation to treat subjects suffering from cardiac inflammation.

Author contributions

A. A. M. is responsible for data curation, formal analysis, investigation, methodology, validation, visualization and writing – original draft preparation; N. I., A. M. H., K. M. L., S. L., R. M. are responsible for data curation, and investigation; D. J. F. is responsible for funding acquisition, resources, writing – review & editing; V. J. V. is responsible for conceptualization, funding acquisition, methodology, project administration, resources, supervision, and writing – review and editing.

Conflicts of interest

VJV and DJF have a patent related to the technology described in this manuscript and are co-founders of Bluegrass Pharmaceuticals Inc.

Data availability

The data that support the findings of this study are available through Open Science Framework (osf.io/xswm4).

Acknowledgements

This work was supported in part by a NIH REACH grant awarded to VJV (U01HL152392) and a NIH Catalyze grant awarded to VJV and DJF (R61HL177474) with additional funding from the University of Kentucky College of Pharmacy for both VJV and DJF. VJV is also supported by grants from the National Institutes of Health (R01HL152081, R01NS116068, and P20GM130456). The authors would like to thank Jilian Cramer and Dali Qian from the University of Kentucky Electron Microscopy Core Facility.

References

1 A. Al-Darraji, D. Haydar, L. Chelvarajan, H. Tripathi, B. Levitan, E. Gao, V. J. Venditto, J. C. Gensel, D. J. Feola and A. Abdel-Latif, *PLoS One*, 2018, **13**, e0200474–e0200425.
2 B. Zhang, W. M. Bailey, T. J. Kopper, M. B. Orr, D. J. Feola and J. C. Gensel, *J. Neuroinflammation*, 2015, **12**, 218.
3 A. Clement, A. Tamalet, E. Leroux, S. Ravilly, B. Fauroux and J.-P. Jais, *Thorax*, 2006, **61**, 895–902.
4 N. Mayer-Hamblett, G. Retsch-Bogart, M. Kloster, F. Accurso, M. Rosenfeld, G. Albers, P. Black, P. Brown, A. Cairns, S. D. Davis, G. R. Graff, G. S. Kerby, D. Orenstein, R. Buckingham, B. W. Ramsey and O. S. Group, *Am. J. Respir. Crit. Care Med.*, 2018, **198**, 1177–1187.
5 B. S. Murphy, V. Sundareshan, T. J. Cory, D. Hayes Jr, M. I. Anstead and D. J. Feola, *J. Antimicrob. Chemother.*, 2008, **61**, 554–560.
6 T. J. Cory, S. E. Birket, B. S. Murphy, C. Mattingly, J. M. Breslow-Deckman and D. J. Feola, *J. Antimicrob. Chemother.*, 2013, **68**, 840–851.
7 D. Amantea, M. Certo, F. Petrelli, C. Tassorelli, G. Micieli, M. T. Corasaniti, P. Puccetti, F. Fallarino and G. Bagetta, *Exp. Neurol.*, 2016, **275**(Pt 1), 116–125.
8 D. Haydar, T. J. Cory, S. E. Birket, B. S. Murphy, K. R. Pennypacker, A. P. Sinai and D. J. Feola, *J. Immunol.*, 2019, **203**, 1021–1030.
9 D. J. Feola, B. A. Garvy, T. J. Cory, S. E. Birket, H. Hoy, D. Hayes Jr. and B. S. Murphy, *Antimicrob. Agents Chemother.*, 2010, **54**, 2437–2447.
10 T. J. Cory, S. E. Birket, B. S. Murphy, D. Hayes Jr, M. I. Anstead, J. F. Kanga, R. J. Kuhn, H. M. Bush and D. J. Feola, *J. Cystic Fibrosis*, 2014, **13**, 164–171.
11 A. Al-Darraji, R. R. Donahue, H. Tripathi, H. Peng, B. M. Levitan, L. Chelvarajan, D. Haydar, E. Gao, D. Henson, J. C. Gensel, D. J. Feola, V. J. Venditto and A. Abdel-Latif, *Sci. Rep.*, 2020, **10**, 16596.
12 J. R. Giudicessi and M. J. Ackerman, *Cleveland Clin. J. Med.*, 2013, **80**, 539–544.
13 V. J. Venditto and D. J. Feola, *Adv. Drug Delivery Rev.*, 2022, **184**, 114252.
14 A. Zizzari, M. Bianco, L. Carbone, E. Perrone, F. Amato, G. Maruccio, F. Rendina and V. Arima, *Materials*, 2017, **10**, 1411.
15 K. Osouli-Bostanabad, S. Puliga, D. R. Serrano, A. Bucchi, G. Halbert and A. Lalatsa, *Pharmaceutics*, 2022, **14**, 1940.
16 C. B. Roces, E. C. Port, N. N. Daskalakis, J. A. Watts, J. W. Aylott, G. W. Halbert and Y. Perrie, *Int. J. Pharm.*, 2020, **586**, 119566.
17 G. M. Whitesides, *Nature*, 2006, **442**, 368–373.
18 S. Joshi, M. T. Hussain, C. B. Roces, G. Anderluzzi, E. Kastner, S. Salmaso, D. J. Kirby and Y. Perrie, *Int. J. Pharm.*, 2016, **514**, 160–168.
19 N. Forbes, M. T. Hussain, M. L. Briuglia, D. P. Edwards, J. H. Ter Horst, N. Szita and Y. Perrie, *Int. J. Pharm.*, 2019, **556**, 68–81.
20 B. Rivnay, J. Wakim, K. Avery, P. Petrochenko, J. H. Myung, D. Kozak, S. Yoon, N. Landrau and A. Nivorozhkin, *Int. J. Pharm.*, 2019, **565**, 447–457.
21 A. A. Masud, F. M. Alsharif, J. W. Creameans, J. Perdeh, D. J. Feola and V. J. Venditto, *Front. Drug Delivery*, 2022, 17.
22 T. Ren, X. Lin, Q. Zhang, D. You, X. Liu, X. Tao, J. Gou, Y. Zhang, T. Yin and H. He, *Mol. Pharm.*, 2018, **15**, 4862–4871.
23 Ž. Vanić, Z. Rukavina, S. Manner, A. Fallarero, L. Uzelac, M. Kralj, D. Amidžić Klarić, A. Bogdanov, T. Raffai, D. P. Virok, J. Filipović-Grčić and N. Škalko-Basnet, *Int. J. Nanomed.*, 2019, 5957–5976.
24 Food and Drug Administration Center for Drug Evaluation and Research, *Guidance for industry: Dissolution testing and acceptance criteria for immediate-release solid oral dosage form drug products containing high solubility drug substances guidance for industry*, FDA, Maryland, 2018.
25 C. B. Roces, G. Lou, N. Jain, S. Abraham, A. Thomas, G. W. Halbert and Y. Perrie, *Pharmaceutics*, 2020, **12**, 1095.
26 C. Webb, N. Forbes, C. B. Roces, G. Anderluzzi, G. Lou, S. Abraham, L. Ingalls, K. Marshall, T. J. Leaver and J. A. Watts, *Int. J. Pharm.*, 2020, **582**, 119266.
27 S. Matschiner, R. Neubert and W. Wohlrab, *Skin Pharmacol. Physiol.*, 1995, **8**, 319–325.
28 X. Cheng and R. J. Lee, *Adv. Drug Delivery Rev.*, 2016, **99**, 129–137.
29 D. Cipolla, H. Wu, S. Eastman, T. Redelmeier, I. Gonda and H.-K. Chan, *Pharm. Res.*, 2016, **33**, 2748–2762.
30 L. Kassaye and G. Genete, *Afr. Health Sci.*, 2013, **13**, 369–375.
31 M. G. Saita, D. Aleo, B. Melilli, S. Mangiafico, M. Cro, C. Sanfilippo and A. Patti, *J. Pharm. Biomed. Anal.*, 2018, **158**, 47–53.
32 ZITHROMAX Package Insert, https://www.pfizermedicalinformation.com: *Pfizer*, 2021.
33 Y.-K. Oh, D. E. Nix and R. M. Straubinger, *Antimicrob. Agents Chemother.*, 1995, **39**, 2104–2111.
34 V. S. Solleti, M. Alhariri, M. Halwani and A. Omri, *J. Antimicrob. Chemother.*, 2015, **70**, 784–796.

35 X. Liu, Z. Li, X. Wang, Y. Chen, F. Wu, K. Men, T. Xu, Y. Luo and L. Yang, *Int. J. Nanomed.*, 2016, **11**, 6781.
36 O. Rajabi, P. Layegh, S. Hashemzadeh and M. Khoddami, *Dermatol. Ther.*, 2016, **29**, 358–363.
37 Z. Rukavina, M. Š. Klarić, J. Filipović-Grčić, J. Lovrić and Ž. Vanić, *Int. J. Pharm.*, 2018, **553**, 109–119.
38 S. Madan, C. Nehate, T. K. Barman, A. S. Rathore and V. Koul, *Drug Dev. Ind. Pharm.*, 2019, **45**, 395–404.
39 H. Aghaei, A. R. S. Nazar and J. Varshosaz, *Colloids Surf., A*, 2021, **614**, 126166.
40 G. Gregoriadis and Y. Perrie, in *Encylcopedia of Life Sciences*, John Wiley & Sons, Ltd., Chichester, 2010, ch. liposomes.
41 S. Geng, X. Liu, H. Xu, C. Cai, Y. Zhang, Q. Yao, H. Xu, J. Gou, T. Yin and W. Xiao, *Expert Opin. Drug Delivery*, 2016, **13**, 337–348.
42 C. T. Uppuluri, P. R. Ravi and A. V. Dalvi, *Int. J. Pharm.*, 2021, **606**, 120881.
43 P. H. Kierstead, H. Okochi, V. J. Venditto, T. C. Chuong, S. Kivimae, J. M. Fréchet and F. C. Szoka, *J. Controlled Release*, 2015, **213**, 1–9.